processes

MDPI

Article

Control the Working Process of the Rotor System with Tilting Pad Bearing

Audrius Čereška

Department of Mechanical and Material Engineering, Faculty of Mechanics, Vilnius Gediminas Technical University (VILNIUS TECH), Plytinės Str. 25, LT-10105 Vilnius, Lithuania; audrius.cereska@vilniustech.lt; Tel.: +370-688-64733

Abstract: Various processes take place in rotor systems with tilting pad bearings. It is important not only to control but also to manage these processes. Due to the instability of the oil film layer in a bearing with inclined pads, oil whirl/whip can occur. Such whirl/whip destabilize the operation of the rotor system. Additional elastic elements between the tilt pads suppress oil whirl/whip and thus reduce rotor vibration excitation. By identifying the working zones of such bearings where oil whirl and whip occur, the problems of rotor rotation instability can be solved. In order to determine the effectiveness of the elastic elements between the tilting pads, research was conducted. A special stand with diagnostic equipment was used for the tests. The clearance between the rotor and the bearing was 50 μm. During the research, the rotor rotation speed was varied from 0 to 5000 rpm. After conducting the research, stable and unstable rotor working zones were determined (Zone I: 0 to 1938 rpm; Zone II: 1938–3923 rpm; Zone III: 3923–5000 rpm). Based on the obtained research results, it is possible to control the working process of the rotor system.

Keywords: rotor system; rotor; tilting pad bearing; rotation speed; control; working process; orbit

Citation: Čereška, A. Control the Working Process of the Rotor System with Tilting Pad Bearing. *Processes* **2024**, *12*, 2583. https://doi.org/10.3390/pr12112583

Academic Editors: Ján Piteľ, Ivan Pavlenko and Sławomir Luściński

Received: 31 May 2024
Revised: 29 July 2024
Accepted: 14 November 2024
Published: 18 November 2024

1. Introduction

Journal bearings are used in various tools, machines, turbochargers, generators, steam turbines, grinding machines, pumps, turbines, fans, cars, ships, and many other mechanisms. However, significantly less research has been devoted to diagnostics and analyses of systems with sliding bearings than to systems with rolling bearings [1–3]. This is due to many reasons. One of the reasons is that it is difficult to use vibro-diagnostic methods because the journal bearings have low vibro-activity [4]. Rotor systems with journal bearings are characterized by unstable operation [5]. Their working vibro-characteristics are very different from the working vibro-characteristics of rolling bearings. If these instabilities occur in the rotor working to a critical resonant rotation speed, the machine's failure is inevitable. This breakdown is sudden, unexpected, and disastrous [6].

In [7], the random parameters that had the greatest effect over the system's stochastic response were determined. This analysis enabled identifying the rotor's rotational frequencies of instability. Nonlinear characteristics are received on their own in the deterministic models. It is necessary to research vibro-diagnostic signals that are difficult to detect in the general background of disturbances [8,9].

In [10], a mechanical model of the circumferentially distributed rods and the nonlinear contact stiffness matrix that characterizes the contact effect between the disks was submitted. The contact stiffness matrix is composed of seven stiffness coefficients that characterize the lateral stiffness, shear stiffness, bending stiffness, and torsional stiffness of the contact interface.

In [11], a new research system for the early detection of oil whirl/whip was presented. Two sensors were used to measure vibrations. A sensor was also installed in the bearing housing to measure the oil whip/whirl.

The essential difference is observed between the rotor vibrations caused by unstable journal bearings, for example, oil whip/whirl, and other excited rotor vibrations, for example, rotor imbalance, temperatures, lubricant film stiffness, etc. [12–16].

The research regarding the stable and unstable causes of rotor rotation is presented in the article in [17].

That article also presents the results of the study of the influence of oil and friction on the stability of rotor rotation.

To avoid fluid-induced instability and high increases in temperature and load capacity inefficiency, in [18], a new concept of a hydrodynamic bearing was proposed in which the bearing's own motion was considered, thus making it possible to change the average velocity of the lubricating oil film inside the bearing. Further, ref. [19] described the effect of a magnetic field applied to a Ferro fluid-lubricated hydrodynamic bearing. A rotor with a single bearing at one end was built to be the test rig. The experimental results showed that three to eight permanent magnets can all increase the instability threshold of the oil bearing. Especially, the magnetic field formed by eight magnets demonstrated an optimal effect. Depending on the number of magnets, oil whirl/whip occurs when the rotor rotation speed is between 3024 and 4480 rpm and from 3184 to 5268 rpm.

In [20], a tilting pad journal bearing was presented whose pads were controlled by electromagnetic actuators. By mounting the electromagnetic actuators in the bearing casing behind the pads, one can exert electromagnetic forces on the pads and make them change their angular position about the bearing. Hence, one can modify the dynamic characteristics of the rotor bearing system for desired and more appropriate values for a given operational condition. The results of the research demonstrated the effectiveness of the system in reducing the lateral vibrations of the rotor during operation, and a good correlation between the numerical and experimental results was observed. In [21], the oil film was shown, which usually becomes unstable, giving rise to a limit-cycle oscillation. The results demonstrate that instability in the oil film does not lead to a simple circular limit-cycle orbit. The whirl/whip-induced limit-cycle oscillations generated by the oil film are more complex and entail coupled circumferential and radial motion. Thus, whirl/whip instability in the oil film may be interpreted as symmetry breaking.

Excited vibrations of tilting pad bearing oil occurred with spontaneous transversal rotor vibrations. These involve self-excited vibrations, when the energy of oil, steam, or gas is transmitted to the rotor. These vibrations arise due to oil whip/whirl [22]. Further, ref. [23] presented the course of the design process and results of numerical and experimental research regarding a prototype microturbine that uses an innovative rotor bearing system. Due to adverse operating conditions, new tilting pad journal bearings were designed in which the sliding surfaces of the tilting pads were composed of polymeric material, and a low-viscosity medium in liquid form was used as the lubricating medium. The results of tests confirmed that the developed bearings performed very well, ensuring the stable operation of the high-speed rotor of the microturbine over a wide speed range.

The purpose of the research in [24] was the theoretical analysis of the journal bearing of a centrifugal pump and the variations in the eccentricity and the rotation of the bearing to detect the instability resulting from oil whirl/whip. Assuming steady and laminar flow, Reynolds theory modified by the Elrod–Adams cavitation model was utilized. In addition, the finite element method (FEM) was used for the theoretical solution. The research results indicated that the pressure on the bearing shell increased considering the effect of the oil whip phenomenon. Control systems have a significant influence on the working processes of rotor bearing systems, including their hydrodynamic and tribological performance. The aim of [25] was to investigate the feasibility of the joint control of rotor vibration and minimizing friction losses in active hybrid bearing (AHB) rotor systems. The theoretical and experimental results indicated that the rotor vibrations were reduced at the energy-efficient operating modes under complex loads.

By knowing the oil parameters of the dynamic system of "rotor–oil–bearing" and the frequency of rotation of the rotor, the operating stability modes of this system can be

determined. When the stable operation modes of the rotor system are exceeded, spontaneous transverse oscillations of the sub-synchronous frequency of the rotor begin, causing oil turbulence in the bearing gaps between the rotor and tilting pads [26–28]. Instability is typical for oil whirls because they increase the dynamic forces and whirl [29–31]. Oil whirl is characterized by instability because of the increased dynamic forces [32–34]. The rotor becomes unstable when the oil cannot maintain the rotor any longer or the whirl frequency coincides with the vibration frequency of the rotor. The latter phenomenon results in excited transversal vibrations of the rotor constant frequency. When the rotor rotates at a certain speed, the amplitude of the transverse vibrations of the rotor reaches an unacceptably high value, which damages the bearings and seals [35]. Stability can be achieved by changing the journal bearing structure using elastic elements [36–39]. Further, ref. [40] presented a novel method for controlling the spindle trajectory by matching the errors between the front and rear bearings. The proposed approach was implemented on a spindle equipped with rolling bearings as the rear support and a hydrostatic bearing as the front support. The proposed technique actively adjusts the amplitude and phase of the spindle trajectory at the hydrostatic bearing to match that of the rolling bearing using piezoelectric ceramic (PZT) membrane restrictors.

In order to increase the rigidity of the tilting pad bearings and rotor rotational stability in a wider speed range, near the journal bearings, bearings of different designs were implemented: elliptical, tilting pads, etc. [41]. The tilting pad bearing has insufficient damping and rotor rotational stability on uneven load distributions between the pads [42,43]. Using elastic elements in the tilting pad bearing [44,45] can change the distribution of the loads between pads, ensuring uniform hydrodynamic film thickness and thus improving the rotation of the rotor rotational stability in the wider rotation speed range. A radial clearance adjustable bearing was proposed in [46]. The structure and working principles of the adjustable bearing were introduced. This adjustable bearing can change the dynamic characteristics of the bearing by adjusting the radial clearance. In that paper, a simple rotor bearing finite element model was used to study the vibration response of the rotor system. When the rotational speed did not reach the critical speed, reducing the radial clearance could effectively reduce the vibration of the rotor, and the vibration suppression effect could reach 67%.

There are many methodologies and data formats, and any of them can be commonly used for the rotating system condition assessment [47]. For a single data format, the result may not always be accurate and reliable. Using multiple data formats simultaneously enables significantly more reliable results to be obtained [30,48].

After conducting a review of the literature, it can be seen that the problem of the work stability of journal bearings is relevant. Various methods have been used to solve the problems of bearing stability: one way is to create new bearing designs or improve the existing ones. The existing solutions and their results are unsatisfactory. In this paper, an adaptive bearing with elastic elements connecting the tilting pads is researched. The research aims to determine the working characteristics of such bearings at various rotor rotation frequencies. The obtained results will be compared with adaptive bearings without elastic elements connecting the tilting pads. The comparison will show the effectiveness of the elastic elements connecting the tilting pads. During the research, three data formats were used to present the results: spectrogram cascades, spectral density graphs, and orbit graphs.

The results obtained during the research can be applied to predict optimal operating modes and failures of rotor systems with tilting pad bearings.

The purpose is to research the oil whip and whirl influence on tilting pad bearings regarding the stability of rotor rotation and determine the stable work zones of the rotor system, as well as to determine the advantages and disadvantages of the application of elastic elements connecting tilting pads of adaptive bearings.

2. Objective of Research

The research objective involves a rotor system with a tilting pad bearing. The tilting pads are linked by elastic elements. The elastic elements in the tilting pads are inserted into

special cavities created in them without any additional fastening. The elastic elements act as a tribological damper and elastic adaptive regulator.

The geometrical parameters of the tilting pad bearing are presented in Table 1.

Table 1. The tilting pad bearing parameters.

Parameter	Size, Unit
Rotor diameter, D	90, mm
Rotor length, L	800, mm
Rotor roundness deviation	1.0–0.2 μm
Rotor linearity deviation	2–3, μm
Rotor hardness, HV	850–1050
Rotor surface roughness, Ra	0.04–0.08, μm
Tilting pad width, L	70, mm
Tilting pad half width, L/2	35, mm
Tilting pad thickness, B	40, mm
Tilting pad angle, β	60°
Tilting pad fastening angle, α	24°30′
Tilting pad roughness, Ra	0.32, μm
The length of the elastic element, L	70, mm
The hardness of the elastic element, HRC	42–48
Density of the elastic element, ρ	7680 kg/m^3 (20 °C), 7660 kg/m^3 (100 °C)
Modulus of elastic element, E	2.12 × 10^{-5} MPa (20 °C), 2.06 × 10^{-5} MPa (100 °C)

The rotor is composed of steel 41CrAlMo7, and the tilting pads are composed of bronze BrT10P1 since bronze has good anti-friction properties compared to steel. The elastic elements between the tilting pads are composed of steel 60MnSiCr4.

The principal construction research of the tilting pad bearing is presented in Figure 1.

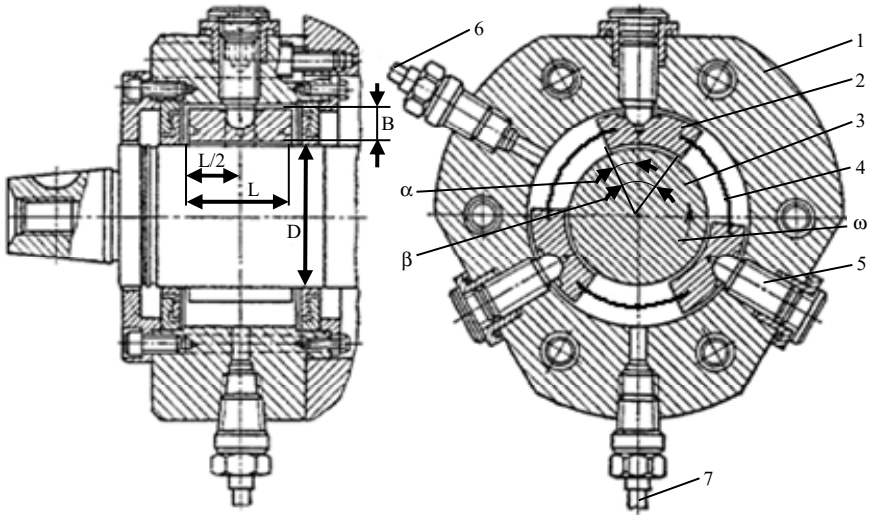

Figure 1. The principal construction of tilting pad bearing with elastic elements between tilting pads: L—tilting pad width; D—rotor diameter; 1—body; 2—tilting pads; 3—rotor; 4—elastic element; 5—adaptive restraint; 6—oil drain nozzle; 7—oil inlet nozzle.

The clearance between the rotor neck and tilting pads as well as the rigidity and damping capacity are controlled by varying the hydrostatic pressure. When vibration is induced, the rigidity and damping capacity of the bearing elements are changed separately for each pad, and, using elastic elements, the bearing adapts to changing conditions and damps the vibrations. These properties of control systems enable damping of vibration and ensure the rotor's rotation at a high degree of accuracy. The rigidity and dissipative characteristics of such tilting pad bearings may be selected depending on the required conditions.

Lubrication is forced. Oil viscosity—6–8 mm^2/s; density ρ—870 kg/m^3 (40 °C); solidification temperature—18 °C; pressure of supplied oil—10–50 kPa.

3. Mathematics of Tilting Pad Bearing Adaptivity

The tilting pad element adaptation and oscillation are ensured by bearing elements of the tilting pads (Figure 2).

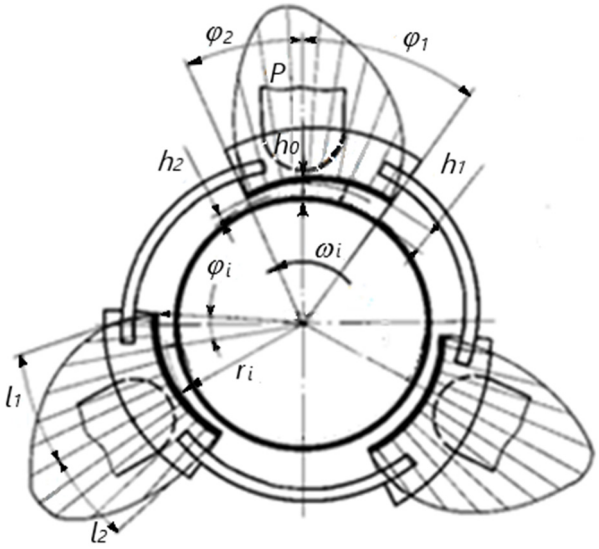

Figure 2. Tilting pad bearing calculation scheme: P—pressure; h_0, h_1, h_2—oil film thicknesses; φ_1, φ_2—tilting pad angles; l_1, l_2—tilting pad lengths; r_i—radius; φ_i—angle; ω_i—rotor angular speed.

The h_0 is determined by the following equation:

$$h_0 = \sqrt{h_1 h_2} \tag{1}$$

where h_1— the thickness of the oil film in the inflow zone; h_2—the thickness of the oil film in the outflow zone.

The oil film between the rotor and tilting pad bearing is wedge-shaped; its thickness is determined by the following equation:

$$h = (r_i + h_1)exp(-tg\theta_n\varphi_i) - r_i \tag{2}$$

The reliability and stability of such a bearing depend largely on the interaction of the elements in the bearing. The interaction of elements is limited by hydrodynamic, tribological, and thermoelastic processes and relationships. This affects the stiffness of the bearing. The initial stiffness of the system is created by damping the elastic elements between the tilting pads. In this case, the angle of inclination of the tilting pads is determined according to the static balance equation:

$$\theta_H^{(j)} = \frac{P^{(j)}B^2(i-1)L}{2C_\theta(i+1)} \tag{3}$$

where $B = l_1 + l_2$, $i = \frac{l_1}{l_2} = \frac{\varphi_1}{\varphi_2}$, L—tilting pad width, j—tilting pad number, and C_θ—stiffness of the elastic element.

The stiffness of the elastic elements is determined by the values of the thickness of the hydrodynamic lubricating film at the inflow and outflow points of the oil under the tilting pad. Stiffness is calculated according to the following equation:

$$2C_\theta = \frac{P^{(j)}B^2(i-1)L}{\left[(i+1)k_{gn}\left(\frac{-1}{\varphi_c}ln\left|\frac{1+h_2}{1+h_1}\right|\right)\right]} \tag{4}$$

where $\varphi_c = \varphi_1 + \varphi_2$; $k_{gn} = \frac{\theta_H}{\theta_n}$.

The selection of stiffness C_θ according to the static criterion $(k_{gn} = 0)$ must be conducted carefully because an unreasonable increase in stiffness reduces the adaptivity of the segments belonging with the dynamic mode, and the elastic element is deformed only from the forced moment and temperature change.

The stiffness of the elastic elements is directly proportional to the hydrodynamic pressure and inversely proportional to the angle of rotation of the tilting pad. The angle of inclination of the wedge-shaped oil layer is determined by the following equation:

$$-tg\theta_n = \frac{dh}{(r_i^2 + h_0)d\varphi_i} \quad (5)$$

When $(\theta_n = 0)$ the oil film has the same thickness.

4. Research Equipment and Methodology

The research system consists of the rotor system for tilting pad bearings: bearing lubrication and refrigeration system; transducers of measurements; boosters; computer; and program packets.

The principal research system structures are presented in Figure 3.

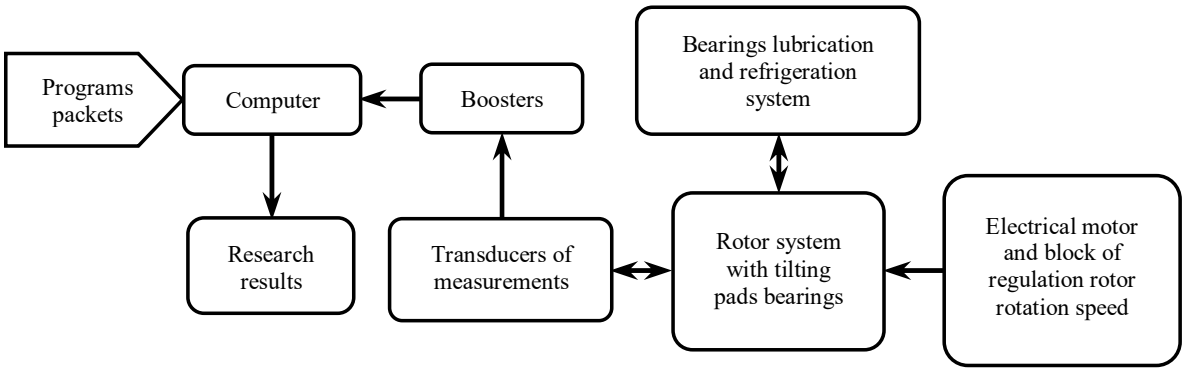

Figure 3. Principal research system scheme.

Principal scheme of experimental stand is presented in Figure 4.

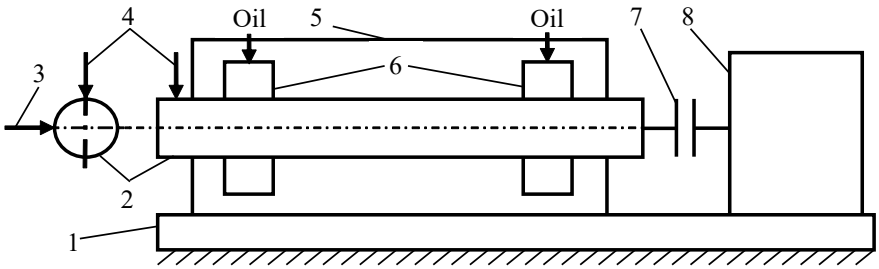

Figure 4. The principal experimental stand scheme: 1—base; 2—rotor; 3—horizontal non-contact transducer of measuring; 4—vertical non-contact transducer of measuring; 5—housing of rotor system; 6—tilting pad bearings; 7—muff; 8—electrical motor.

The experimental stand photograph is presented in Figure 5a. The measuring between transducers must be 90-degree angle. To measure the accuracy of the rotor's rotation, used Hottinger Baldwin Messtechnik (HBM) two non-contact induction displacement transducers model Tr 102 and (HBM) booster model KWS 503D (Hottinger Brüel & Kjaer GmbH, Darmstadt, Germany). A coupling with two half-couplings connected by two fingers was used. Dimensions: diameter D—80 mm; length L—100 mm. An elastic material was placed on the fingers so that the contact between the two halves is elastic. Before the

measurements, the coupling was adjusted so that it would not affect the measurement results. The principal measurement scheme is presented in Figure 5b.

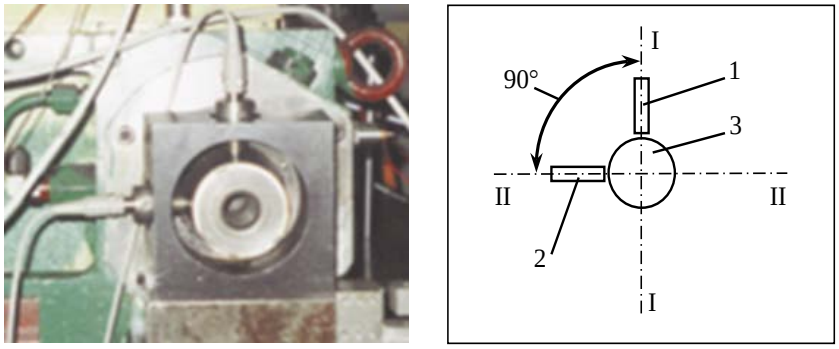

(**a**) (**b**)

Figure 5. Experimental stand: (**a**) photograph; (**b**) principle scheme of the arrangement of measuring transducers: I–I—position of vertical; 1—vertically mounted non-contact transducer; II–II—position of horizontal; 2—horizontally mounted non-contact transducer of measuring; 3—rotor.

Regulation and calibration of the equipment were performed prior to the research. The research was carried out according to the scheme presented in Figure 3.

The research results were analyzed using computer programs (Origin, Master Data, Excel, Excel, Statistics, etc.). The primary measurement results (rotor vibration displacements) were analyzed mathematically (e.g., Fourier function transformation (FFT), etc.). Domain formats obtained after the analysis are needed to evaluate the quality of the rotor system work (spectrogram cascades, orbits, vibration spectrum, etc.).

The primary clearance between the rotor neck and bearing tilting pads is 50 μm. Change in oil temperature during the experiment 20 °C–75 °C. During the experiment, the rotor speed was changed every 500 rpm from 0 to 5000 rpm.

5. Results of Analysis and Discussion

Three data formats were applied in the research: spectrogram cascade, spectral density, and orbit. The spectrogram-cascade graph of the researching rotor system is provided below (Figure 6).

From the spectrogram-cascade graph (Figure 6), it can be seen that the rotor rotates steadily from 0 to 1938 rpm (I zone). When exceeding 1938 rpm, spontaneous vibrations of the rotor appear, and that effect continues until the rotation speed reaches 3923 rpm (II zone). No spontaneous vibrations are observed when the rotor rotation is in the range 3923–5000 rpm (III zone).

From the research results of bearings [29–31,49,50], it can be seen that adaptive bearings without tilting pads connecting the elements have two oil whirl zones and a whip zone. The first oil whirl stage starts when the rotor rotates at 2500–3500 rpm, the second oil whirl stage starts from 4000 rpm and continues to 6500 rpm, and, from 6500 rpm, the oil whip starts. After comparing the spectrogram-cascade graphs of tilting pad bearings with journal bearings, the tilting pad bearings were more stable in a wider range of rotation speed, not only because there was only oil whirl but because there was no oil whip. This confirms that the elastic elements connecting the tilting pads are effective and meaningful. The application of adaptive bearings with elastic elements is useful, although the design and adjustment of these bearings are more complicated.

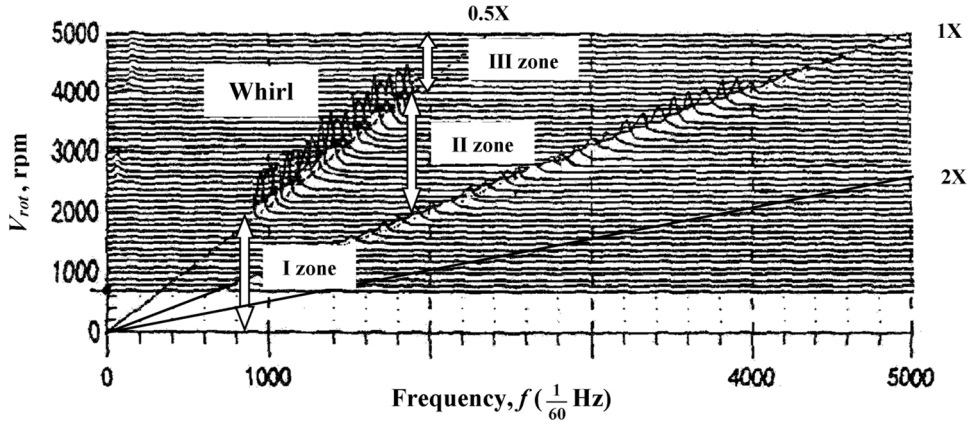

Figure 6. Rotor system spectrogram-cascade graph when rotor rotation speed is 0–5000 rpm: I zone (range 0–1938 rpm), II zone (range 1938–3923 rpm), and III zone (range 3923–5000 rpm).

After the primary measurement results, Fourier function transformation (FFT) was conducted, as indicated in the rotor vibration spectrum graph (Figure 7). It can be seen that the critical speed frequency of the researched system is obtained by a rotor rotation speed of 3300 rpm.

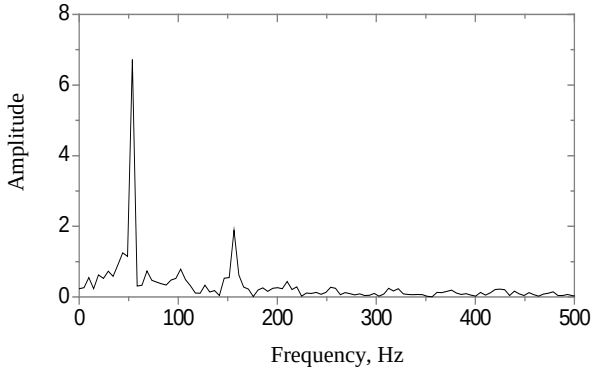

Figure 7. Rotor vibration spectrum.

The orbits of the rotor rotation axis depending on the rotation of the rotor rotation speed are provided in Figures 8–13. Evidently, the information of the orbits is highly correlated with the rotor vibration spectrum and the spectrogram-cascade graph results.

When the rotor rotation speed is 2000 rpm (Figure 8), the orbital form is irregular and chaotic because the range of oil whirl can reach up to 2500 rpm (Figure 9). Although the effect of oil whip is visible, the orbit slightly stabilizes and its form begins to approach a regular circle. When the rotor rotation speed is 3000 rpm (Figure 10), the form of the orbit is unstable and irregular; beyond the resonant frequency, the orbit starts to stabilize again, which can be viewed in the rotor rotation speed orbit at 3500 rpm (Figure 11). At the end of a zone of whirl and with rotor rotation at 4000 rpm (Figure 12), the orbit is further approaching an ideal circle form and the thickness of the outer ring of the orbit decreases.

When there is no oil whirl/whip, the form of the orbit (Figure 13) becomes more regular and elliptical. This means that the rotor rotates more precisely and more evenly. This means that the oil has a minimum of beating, which is confirmed by the graph of the spectrogram cascade (Figure 6). The diameter of the orbit circle is also decreased.

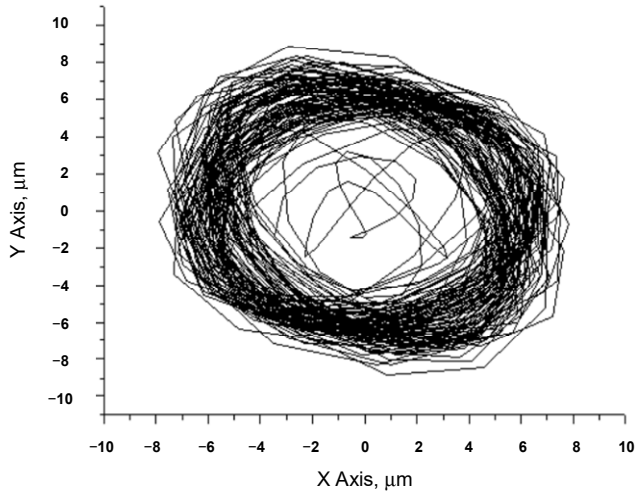

Figure 8. Rotor rotation orbit when rotor rotation speed is 2000 rpm.

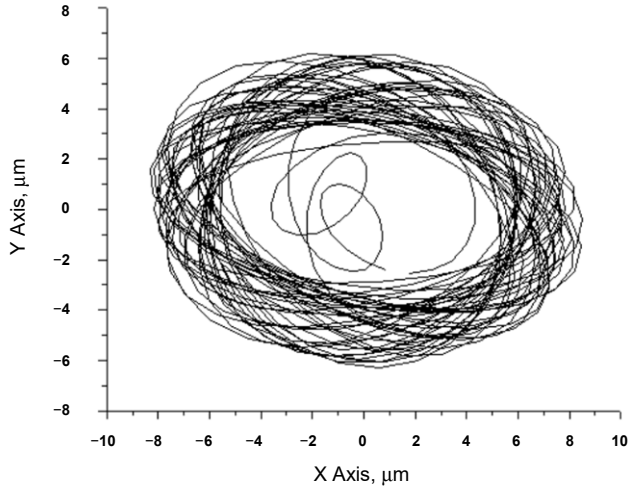

Figure 9. Rotor rotation orbit when rotor rotation speed is 2500 rpm.

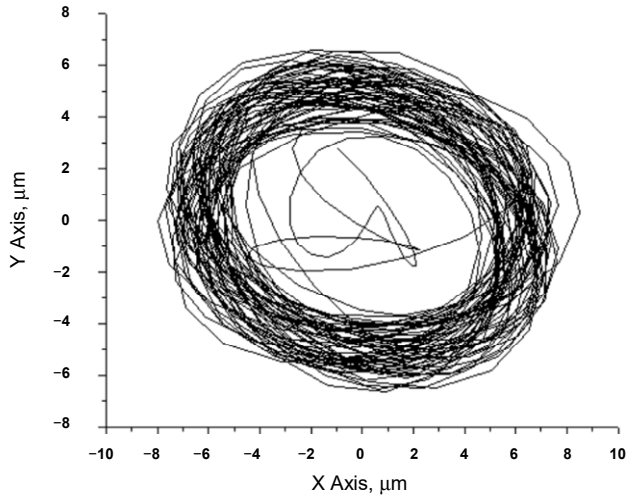

Figure 10. Rotor rotation orbit when rotor rotation speed is 3000 rpm.

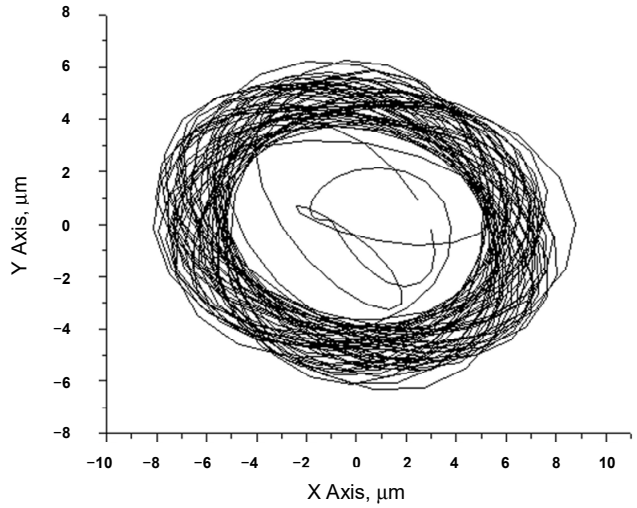

Figure 11. Rotor rotation orbit when rotor rotation speed is 3500 rpm.

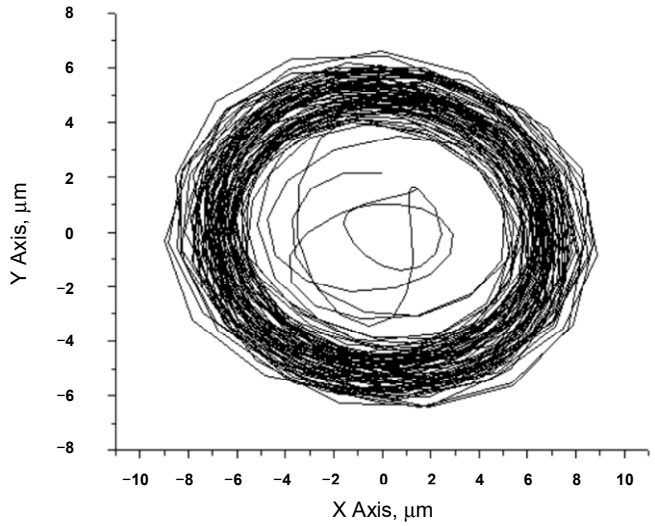

Figure 12. Rotor rotation orbit when rotor rotation speed is 4000 rpm.

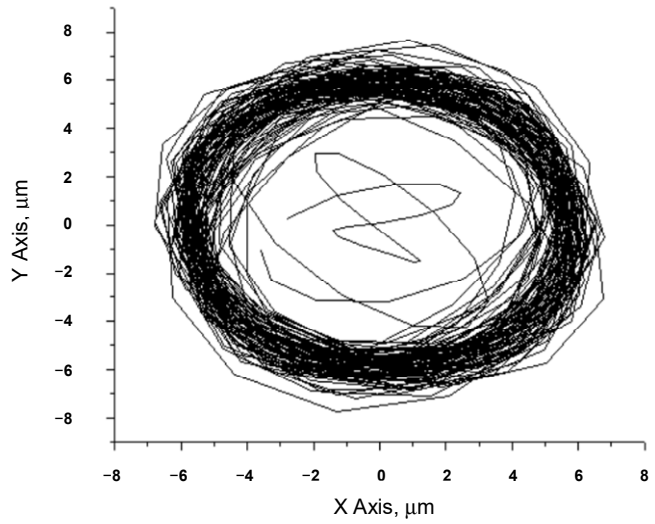

Figure 13. Rotor rotation orbit when rotor rotation speed is 4500 rpm.

The ideal case would be if the rotor axis would not move as the rotor rotates, but deviation is inevitable. The purpose is that the rotor axis orbit maximally approaches the ideal circle form.

Research shows that such bearings have both advantages and disadvantages.

Advantages: Bearings with tilting pads are adjustable, so, when changing the gap between the rotor and tilting pads, the parameters of the rotor system change: stiffness, resonance frequency, whirl/whip, etc., which means that the application possibilities of the bearings increase.

Disadvantages: Complex installation, tuning, management, etc.

The advantages outweigh the disadvantages, meaning that these bearings are suitable for use in a wide range of industrial applications and require further research and design improvements.

6. Conclusions

It is evident under the spectrogram-cascade graph that the rotor system with a tilting pad bearing rotor rotating speed in the range from 0 to 5000 rpm has three work zones:

- I zone: 0–1938 rpm—zone of stable work.
- II zone: 1938–3923 rpm—rotor rotation critical zone because the rotor is exposed to oil whirl.
- III zone: 3923–5000 rpm—zone of stable work.

The resonant rotor rotation speed is when the rotor rotation speed reaches 3300 rpm. This means that, with such bearings, such a rotor rotation speed must be strictly avoided.

In the researched tilting pad bearing rotor rotation range from 0 to 5000 rpm, there is oil whirl only and there is no oil whip.

Bearings of different designs have different oil whirl/whip ranges depending on the rotor's rotation speed and other factors.

The research results confirm that adaptive bearings with tilting pads are effective and meaningful. Bearings with tilting pads work stably, but the additional application of elastic elements between the tilting pads increases the stability of the rotor system. The application of adaptive bearings with elastic elements is useful, although the design and adjustment of these bearings are more complicated.

The rotation orbit of the rotor axis is a significantly more informative data format than other data formats. Therefore, it is recommended to apply formats by conducting research.

The presented research methodology can be used to research other bearings of similar designs.

Numerical modeling of these bearings is planned in the future. The comparative analysis data from the numerical simulation and experimental research results will provide more information on the control and management of these bearings. Then, the possible applications of these bearings will become even broader. Also, it is planned to compare tilting pad bearings without connecting and with connecting elastic elements.

Funding: This research received no external funding.

Data Availability Statement: The data that support the findings of this research are available from the author upon reasonable request.

Conflicts of Interest: The author declares no conflicts of interest.

References

1. Allmaier, H.; Priestner, C.; Six, C.; Priebsch, H.H.; Forstner, C.; Novotny-Farkas, F. Predicting friction reliably and accurately in journal bearings-a systematic validation of simulation results with experimental measurements. *Tribol. Int.* **2011**, *44*, 1151–1160. [CrossRef]
2. Dimond, T.; Younan, A.; Allaire, P. A review of tilting pad bearing theory. *Int. J. Rotating Mach.* **2011**, *2011*, 908469. [CrossRef]
3. Vannini, G.; Cangioli, F.; Ciulli, E.; Nuti, M.; Forte, P.; Kim, J.; Livermore-Hardy, R. Experiments on a Large Flexure Pivot Journal Bearing: Summary of Test Results and Comparison With Predictions. *J. Eng. Gas Turbines Power* **2020**, *142*, 031004. [CrossRef]

4. Liu, S.; Xiao, Z.; Yan, Z.; Chen, Z. Vibration characteristics of rotor system with tilting-pad journal bearing of elastic and damped pivots. *J. Cent. South Univ.* **2015**, *22*, 134–140. [CrossRef]
5. Ondrouch, J.; Ferfecki, P.; Poruba, Z. Active vibration reduction of rigid rotor by kinematic excitation of bushes of journal bearings. *Metalurgija* **2010**, *49*, 107–110.
6. Tejas, H.P.; Darpe, A.K. Vibration response of a cracked rotor in presence of rotor–stator rub. *J. Sound Vib.* **2008**, *317*, 841–865. [CrossRef]
7. Garoli, G.Y.; de Castro, H.F. Analysis of a rotor-bearing nonlinear system model considering fluid-induced instability and uncertainties in bearings. *J. Sound Vib.* **2019**, *448*, 108–129. [CrossRef]
8. Bently, D.E. Rotating Machinery Measurements 101. *Orbit* **1994**, *15*, 4–6.
9. San, A.L.; Koo, B.; Hemmi, M. A Flow Starvation Model for Tilting-Pad Journal Bearings and Evaluation of Frequency Response Functions: A Contribution Toward Understanding the Onset of Low Frequency Shaft Motions. *J. Eng. Gas Turbines Powder Trans. ASME* **2018**, *140*, 052506. [CrossRef]
10. Wu, X.L.; Jiao, Y.H.; Chen, Z.B.; Ma, W.S. Establishment of a contact stiffness matrix and its effect on the dynamic behavior of rod-fastening rotor bearing system. *Arch. Appl. Mech.* **2021**, *91*, 3247–3271. [CrossRef]
11. Safizadeh, M.S.; Golmohammadi, A. Prediction of oil whirl initiation in journal bearings using multi-sensors data fusion. *Measurement* **2020**, *151*, 107241. [CrossRef]
12. Ryu, K.; Ashton, Z. Bump-Type Foil Bearings and Flexure Pivot Tilting-Pad Bearings for Oil-Free Automotive Turbochargers: Highlights in Rotordynamic Performance. *J. Eng. Gas Turbines Powder Trans. ASME* **2016**, *138*, 042501. [CrossRef]
13. Tong, X.; Palazzolo, A. Measurement and Prediction of the Journal Circumferential Temperature Distribution for the Rotordynamic Morton Effect. *J. Tribol. Trans. ASME* **2018**, *140*, 031702. [CrossRef]
14. Galvao, M.M.; Menon, G.J.; Schwarz, V.A. Numerical study of the influence of the pivot position on the steady-state behavior of tilting-pad thrust bearings. *J. Braz. Soc. Mech. Sci. Eng.* **2017**, *39*, 3165–3180. [CrossRef]
15. Hagemann, T.; Zeh, C.; Proelss, M.; Schwarze, H. The Impact of Convective Fluid Inertia Forces on Operation of Tilting-Pad Journal Bearings. *Int. J. Rotating Mach.* **2017**, *2017*, 5683763. [CrossRef]
16. Wang, L.; Fu, Y.; Pei, S.; Xu, H. Theoretical and Experimental Study on the Axial Oil Film Stiffness of Tilting-Pad Thrust Bearings. *Tribol. Trans.* **2017**, *60*, 419–427. [CrossRef]
17. Fan, C.C.; Syu, J.W.; Pan, M.C.; Tsao, W.C. Study of start-up vibration response for oil whirl, oil whip and dry whip. *Mech. Syst. Signal Process.* **2011**, *25*, 3102–3115. [CrossRef]
18. Ramos, D.J.; Daniel, G.B. A new concept of active hydrodynamic bearing for application in rotating systems. *Tribol. Int.* **2021**, *153*, 106592. [CrossRef]
19. Luo, L.Y.; Fan, Y.H.; Tang, J.H.; Chen, T.Y.; Zhong, N.R.; Feng, P.C.; Kao, Y.C. Frequency Enhancement of Oil Whip and Oil Whirl in a Ferrofluid–Lubricated Hydrodynamic Bearing–Rotor System by Magnetic Field with Permanent Magnets. *Appl. Sci.* **2018**, *8*, 1687. [CrossRef]
20. Silva, H.A.P.; Nicoletti, R. Rotor vibration control using tilting-pad journal bearing with active pads — Numerical and experimental results. *J. Sound Vib.* **2023**, *546*, 117441. [CrossRef]
21. Schweizer, B. Oil whirl, oil whip and whirl/whip synchronization occurring in rotor systems with full-floating ring bearings. *Nonlinear Dyn.* **2009**, *57*, 509–532. [CrossRef]
22. Ding, A.; Ren, X.; Li, X.; Gu, C. Numerical Investigation of Turbulence Models for a Superlaminar Journal Bearing. *Adv. Tribol.* **2018**, *2018*, 2841303. [CrossRef]
23. Zywica, G.; Olszewski, A.; Baginski, P.; Andrearczyk, A.; Zochowski, T.; Klonowicz, P. Theoretical analysis and experimental tests of tilting pad journal bearings with shoes made of polymer material and low-boiling liquid lubrication. *Tribol. Int.* **2023**, *189*, 108991. [CrossRef]
24. Hekmat, M.H.; Biukpour, G.A. Numerical study of the oil whirl phenomenon in a hydrodynamic journal bearing. *J. Braz. Soc. Mech. Sci. Eng.* **2019**, *41*, 218. [CrossRef]
25. Li, S.; Zhou, C.; Savin, L.; Shutin, D.; Kornaev, A.; Polyakov, R.; Chen, Z. Theoretical and experimental study of motion suppression and friction reduction of rotor systems with active hybrid fluid-film bearings. *Mech. Syst. Signal Process* **2023**, *182*, 109548. [CrossRef]
26. Chasalevris, A.; Sfyris, D. Evaluation of the finite journal bearing characteristics, using the exact analytical solution of the Reynolds equation. *Tribol. Int.* **2013**, *57*, 216–234. [CrossRef]
27. Liu, H.; Xu, H.; Ellison, P.J.; Jin, Z. Application of computational fluid dynamics and fluid-structure interaction method to the lubrication study of a rotor-bearing system. *Tribol. Lett.* **2010**, *38*, 325–336. [CrossRef]
28. Tong, X.A.; Palazzolo, A.; Suh, J. Review of the Rotordynamic Thermally Induced Synchronous Instability (Morton) Effect. *ASME Appl. Mech. Rev.* **2017**, *69*, 060801. [CrossRef]
29. Muszynska, A.; Bently, D.E. Fluid-induced instabilities of rotors: Whirl and whip—Summary of results. *Orbit* **1996**, *17*, 7–15.
30. Muszynska, A. Alford and the destabilizing forces that lead to fluid whirl/whip. *Orbit* **1998**, *19*, 29–31.
31. Muszynska, A.; Hatch, C.T. Oil whip of a rotor supported in a poorly lubricated bearing. *Orbit* **1998**, *19*, 4–8.
32. Wang, W.M.; Liu, B.B.; Zhang, Y.; Shao, X.; Allaire, P.E. Theoretical and experimental study on the static and dynamic characteristics of tilting-pad thrust bearing. *Tribol. Int.* **2018**, *123*, 26–36. [CrossRef]

33. Shen, J.; Xiong, X.; Li, G.; Wang, X.; Hua, Z.; Nie, Z. Experimental Analysis of Dynamic Oil Film Pressure of Tilting-Pad Journal Bearings. *Tribol. Lett.* **2016**, *63*, 36. [CrossRef]
34. Grigor'ev, B.S.; Fedorov, A.E. A New Improved Method for Calculating Dynamic Coefficients of Fluid Film Bearings. *J. Mach. Manuf. Reliab.* **2016**, *45*, 59–64. [CrossRef]
35. Muszynska, A. Vibrational diagnostics of rotating machinery malfunctions. *Int. J. Rotating Mach.* **1995**, *1*, 237–266. [CrossRef]
36. Marcinkevičius, A.H. Automatic regulation of clearance in a tilting pad journal bearing. *Mechanika* **2012**, *18*, 192–195. [CrossRef]
37. Marcinkevičius, A.H.; Jurevičius, M. Automatic Control of Loading Forces in a Tilting Pad Journal Bearing. *Hindawi Publ. Corp. Adv. Mech. Eng.* **2014**, *6*, 590695. [CrossRef]
38. Tong, X.; Xu, W.; Shi, Y.; Cai, M.; Palazzolo, A. Transient rotordynamic thermal bow (Morton effect) modeling in flexure-pivot tilting pad bearing systems. *Tribol. Int.* **2023**, *177*, 107954. [CrossRef]
39. Rodriguez, L.E.; Childs, D.W. Frequency dependency of measured and predicted rotordynamic coefficients for a load-on-pad flexible-pivot tilting-pad bearing. *J. Tribol.* **2006**, *128*, 388–395. [CrossRef]
40. Zhang, Y.; Pan, W.; Chen, S.; Lu, C.; Zhang, Y. Research on trajectory control of rotor systems supported by a combination of rolling and hydrostatic bearings. *Precis. Eng.* **2024**, *88*, 475–486. [CrossRef]
41. Carbonara, A.F.; Duarte, D., Jr.; Bittencourt, M.L. Comparison of journal orbits under hydrodynamic lubrication regime for traditional and Newton-Euler loads in combustion engines. *Lat. Am. J. Solids Struct.* **2009**, *6*, 13–33.
42. Hargreaves, D.J.; Fillon, M. Analysis of a tilting pad journal bearing to avoid pad fluttering. *Tribol. Int.* **2007**, *40*, 607–612. [CrossRef]
43. Wang, Z.; Liu, Y.; Wang, Y.; Liu, X.; Wang, Y. Influence of squeezing and interface slippage on the performance of water-lubricated tilting-pad thrust bearing during start-up and shutdown. *Lubr. Sci.* **2018**, *30*, 137–148. [CrossRef]
44. Gropper, D.; Harvey, T.J.; Wang, L. Numerical analysis and optimization of surface textures for a tilting pad thrust bearing. *Tribol. Int.* **2018**, *124*, 134–144. [CrossRef]
45. Suh, J.; Palazzolo, A. Numerical modeling and analysis of flexure-pivot tilting-pad bearing. *J. Tribol.* **2017**, *139*, 051704. [CrossRef]
46. Zhang, L.; Xu, H.; Zhang, S.; Pei, S. A radial clearance adjustable bearing reduces the vibration response of the rotor system during acceleration. *Tribol. Int.* **2020**, *144*, 106112. [CrossRef]
47. Barzdaitis, V.; Cinikas, G. Condition monitoring data formats used in rotating machinery diagnostics. *Mechanika* **1997**, *2*, 40–48.
48. Vasylius, M.; Didžiokas, R.; Mažeika, P.; Barzdaitis, V. The rotating system vibration and diagnostics. *Mechanika* **2008**, *72*, 54–58.
49. Bently, D.E.; Muszynska, A. Role of Circumferential Flow in the Stability of Fluid-Handling Machine Rotors. In Proceedings of the Fifth Workshop on Rotordynamics Instability Problems in High Performance Turbomachinery, Texas A&M University, College Station, TX, USA, 16–18 May 1988.
50. Tuma, J.; Biloš, J. Fluid Induced Instability of Rotor Systems with Journal Bearings. *Eng. Mech.* **2007**, *14*, 69–80.